HEFAT2012
9th International Conference on Heat Transfer, Fluid Mechanics and Thermodynamics
16 – 18 July 2012
Malta

EXPERIMENTAL INVESTIGATION OF FLOW AND FORCED CONVECTION HEAT TRANSFER, IN FULLY FILLED RECTANGULAR DUCT USING POROUS MEDIA

Shokouhmand H.* and Emami S.M.
*Author for correspondence
Faculty of Engineering Mechanical Engineering Dept.
University of Tehran,
Tehran, 1439957131,
Iran,
E-mail: mehrdademami@ut.ac.ir

ABSTRACT

An experimental study was performed to investigate the heat transfer characteristics of the convection flow through a rectangular air duct with aspect ratio of 10 (a/b=10) which is filled with metallic porous materials. All four walls of the duct are subjected to a constant and uniform heat flux. The Reynolds number based on the hydraulic diameter has been kept between 500-2000 in order to ensure the laminar flow through the duct. The effect of different parameters such as variable porosity and density of porous layers have been investigated. For different porous layers configuration, heat flux at the walls, wall temperatures and air mass flow rate has been measured and the Nusselt number has been calculated. The results are compared with the clear flow case where no porous material was used. It can be concluded that higher heat transfer rates can be achieved in porous media flow case at the expense of a reasonable pressure drop. Based on the experimental data new empirical correlations for both Nusselt number and friction factor have also been developed for such air duct, which gives a good agreement between predicted values and experimental values of Nusselt number and friction factor.

INTRODUCTION

Theoretical and applied researches in flow and heat transfer in porous media have received more attention during the past three decades. This is due to the importance of this research area in many engineering applications such as solid matrix heat exchangers, heat pipes, drying efficiency, electronic cooling, enhanced heat transfer by surface modification, nuclear reactors using gaseous coolants flowing through radioactive pellets, dehumidifying, Porous preheaters and flame stabilizers, oil and gas flow in reservoirs, catalytic converter for air pollution reduction of combustion products, etc.

Kays and London [1] pointed out that an effective way to increase the performance of a heat exchanger is to increase its surface area to volume ratio. Kim et al. [2] established correlations for friction factor and overall heat transfer coefficient for metal foam channel heat exchangers via experimental techniques. Edouard et al. [3] examined the effect of morphology of the foam (struts and pores diameter, exchange specific surface area, etc.) in the prediction of bed permeability for different types of solid foams experimentally and theoretically. Hsu et al. [4] and Hsu and Fu [5] measured the velocity and the pressure drop for both steady and oscillating flows across porous columns packed from wire screens. Mohamad [6] suggested a novel type of solar air heater which combines double air passage and porous absorber plate, and Alvarez et al. [7] developed and tested an efficient single-glass air solar collector with an absorber plate made of recyclable aluminum cans (RAC). Varshney and Saini [8] have experimentally investigated the heat transfer and the fluid flow characteristics of a solar air heater having its duct packed with wire mesh screen matrices (air flowing parallel to matrix planes). Lee and Vafai [9] developed an analytical solution for temperature distribution within a channel filled with a porous medium and subject to a constant heat flux boundary condition. They established an analytical relationship for Nusselt number as a function of solid and fluid effective thermal conductivities and solid–fluid interfacial characteristics utilizing local thermal non-equilibrium model.

Open cell porous matrix such as an unconsolidated bed of small particles, woven metal screens, or foam matrixes provides excellent heat-transfer characteristics due to its large surface area to volume ratio. Woven metal screens have other advantages include easy arrangement, high permeability and relatively small deviation of the pore size from the mean value.

Present experimental study includes the heat transfer and pressure drop investigations of the flow passing through a rectangular channel in which different porous media are located. All four walls of the channel are heated by uniform heat flux about 174 W/m². The experiments were carried out for Reynolds numbers (based on the hydraulic diameter) between 500-2000, and 3 different porous media, which their porosities varied

between 95% and 98%, were examined. The maximum increase in the length-averaged value of the Nusselt number of about 4.9 times in comparison with the clear flow case was achieved with a porous medium fully filled the duct (porosity 98% and a Reynolds number of about 2000). Using experimental data, two correlations have been developed for predicting the Nusselt number and friction factor for such rectangular air ducts. Comparison of the empirical correlations with experimental data in open literature validated the empirical correlations.

NOMENCLATURE

A	[m^2]	*Area*
C_P	[J/kg K]	Specific heat at constant pressure
Da	[-]	Darcy number
D_h	[m]	Hydraulic diameter
D_p	[m]	Equivalent spherical diameter
f_{Dp}	[-]	Modified Fanning friction factor
F	[-]	Inertial coefficient
h	[W/ m^2K]	Convective heat transfer coefficient
H	[m]	Channel height
K	[m^2]	Permeability
k	[W/mK]	Thermal conductivity
L	[mm]	Distance between two adjacent screens
L_0	[m]	Length of test section
$\dot{m}$	[kg/s]	Mass flow rate
$\overline{Nu}_{D_h}$	[-]	Average Nusselt number based on the hydraulic diameter
P	[m]	Wetted Perimeter of the test section
Δp	[Pa]	Pressure drop
q	[W/ m^2]	Local wall heat flux
Q	[W]	Heat transfer rate
Re	[-]	Reynolds number
S_v	[m^{-1}]	Surface area per unit volume of solid phase
T	[K]	Temperature
$\overline{T}$	[K]	Average surface temperature
u	[m/s]	Air velocity

Special characters

α	[-]	Unknown coefficient
β	[-]	Unknown coefficient
γ	[-]	Unknown coefficient
ε	[-]	Porosity
μ	[kg/m s]	Viscosity
ρ	[kg/ m^3]	Density

Subscripts

air	Air
c	Cross section of test section
D_h	Based on hydraulic diameter
D_p	Based on equivalent spherical diameter
in	At test section inlet
m	mean
out	At test section outlet
s	Heated surface of test section

EXPERIMENTAL STUDY

Setup and procedure

The schematic diagram of test setup is shown in Figure 2. The setup includes the test section, flat heater, centrifugal fan and instrumentations for measuring mass flow rate of air, pressure drop, temperature and voltage for heating the test section. Air from the quiescent laboratory room is driven into the operators by means of a downstream-positioned fan (8). The air enters a long hydrodynamic development length (1.2 m), (1) and (2), in order to establish a well-defined velocity profile at its downstream end. The downstream end of the development section is mated to the inlet of the test section (3). The test section is a rectangular duct with cross-sectional aspect ratio of 10, filled with a metallic porous matrix (figure 1). The length of the test section in the flow direction is 0.5 m. The downstream end of the test section is mated to the exit section (4) that is an extension of the test section walls, but without the porous medium. The inlet of the exit section was equipped with honeycomb straighter for uniforming the flow field. The exit section was followed by a mixing device (5), namely baffles for mixing the air. The mixing device enabled measurement of the bulk mean temperature at the outlet of the test section. The length of the exit section was 0.35 m and its cross section area matched with that of the test duct. Three equally spaced baffle plates which spread over 0.0425 m length beyond the exit section were provided for the purpose of mixing the hot air coming out of the test section to obtain a uniform temperature of the air at the outlet. The mixing section was connected to the pipe fitting (7) through a transition piece and flexible pipes (6). At the far end of the air velocity measurement pipe, an isolation device was installed to decouple any possible blower-motor vibration.

Heating of test section was accomplished on all of its bounding surfaces by means of a flat heater. The heater plates consist of asbestos sheet, mica and nichrome wires. The wires were fixed on asbestos sheet covered with strips of mica to keep the uniform distance between the wires. The heater was fabricated to produce about 2000 W/m^2 heat energy. With the help of a voltage regulator, a voltage of 65 V across the wires having total resistance of 54 Ω was maintained. Corresponding to this voltage of 65 V and resistance of 54 Ω, about 78 W of energy over a surface area of 0.45 m^2 was obtained. All of the outer bounding surfaces of heater and exit section were carefully wrapped with a 0.038 m thick rock wool (k = 0.03 W/m K) as insulating material to minimize the extraneous heat losses.

Temperatures were measured by thermocouples deployed along the centre span of the walls of the test section and its upstream and downstream extensions. The thermocouples (Type J, 0.3-mm-diameter) had been specifically calibrated after their installation ($\pm 0.1\,^{\circ}C$). At all thermocouple locations, the thermocouple junctions were pressed tightly against the outer surface of the respective walls. Using 20 thermocouples, temperatures of all four surfaces of the test section, at five axial positions (0.020, 0.135, 0.250, 0.365 and 0.480 m) were measured. In addition, three thermocouples were used to measure the fluid bulk temperature, respectively positioned upstream and (among the baffles of) downstream of the heated test section. The thermocouples outputs were displayed in $^{\circ}C$, by Hanyoung- ED6 temperature meters.

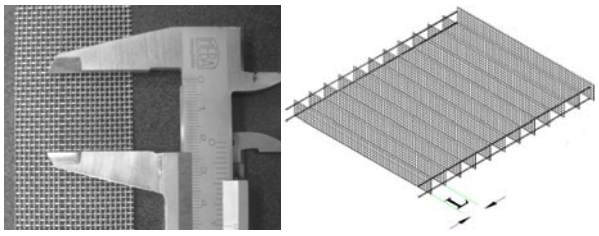

Figure 1 Porous material

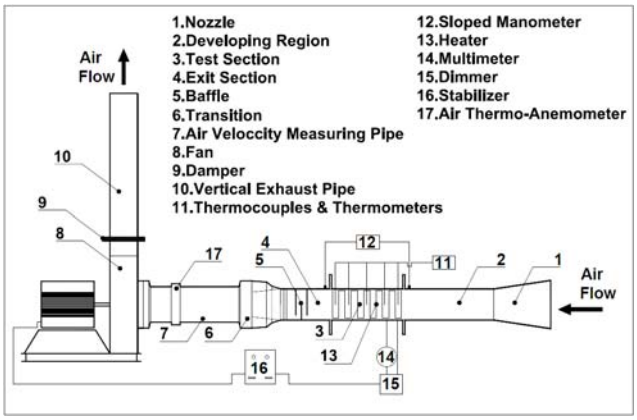

Figure 2 Experimental setup

The pressure drop across the test section has been measured by a sloped manometer having 0.01 mm accuracy. The liquid having density of 784 kg/m^3 at $29\,°C$ has been used in manometer to further increase the accuracy.

For the measurement of the mass flow rate, a dedicated instrumented section (7), situated downstream of the exit section, was used. The instrumented section had been previously calibrated against a rotameter and determines temperature and flow rate of air through the tube internal diameter 60 mm, hence by having flow rate, temperature and flow surface, the mass flow of air be calculated by the device.

The porous media used for experiments were manufactured from commercial steel screens (wire diameter 0.45×10^{-3} m, density 7830 kg/m^3, thermal conductivity 64 W/mK) which cut into a rectangular shape with dimension of 0.4×0.04 m^2 are packed layer by layer in the 0.5 m long test section. Three different porous media, whose properties are presented in Table 1, were obtained by varying the distance between two adjacent screens L.

Table 1
Porous media characteristics

Porous medium	Screen Dimension (mm)²	L (mm)	ε (%)	K (m²)	F	D_p	$Da=\frac{K}{(H/2)^2}$
(1)	40×400	2	95	2.88×10^{-7}	4.69×10^{-2}	2.45×10^{-3}	7.20×10^{-4}
(2)	40×400	4	97	3.23×10^{-7}	2.81×10^{-2}	2.45×10^{-3}	8.07×10^{-4}
(3)	40×400	6	98	4.13×10^{-7}	2.01×10^{-2}	2.45×10^{-3}	1.03×10^{-4}

All joints of duct, inlet section, test section, exit section, transition and pipes are thoroughly checked up for any leakage each time before starting the experiment. All the measuring equipments were checked up before starting the experiment. Usually an initial period of approximately 3–4 h was required before reaching steady-state conditions (considered to be attained, when the temperatures indicated by the thermocouples did not vary with more than $\pm0.3\,°C$ within a period of about 20 min). Following parameters were measured for each set of readings: pressure drop across the test section, temperatures of the test section walls, the fluid bulk temperature at inlet and outlet of the test section, voltage and electric current supplied to heater, air velocity and temperature at the air velocity measurement pipe, to measure the air flow rates. After collecting a set of data at steady-state conditions, the mass flow rate of air was increased so that the next value of the Re number differed from the previous one by about 250 units. A new set of data was collected when steady-state conditions were reached again, usually within a period of approximately 40 min. That is, the mass flow rate of air was increased progressively until a maximum value of Re ~ 2000 was reached.

In order to verify the validity of the experimental setup the values of Nusselt number and friction factor were compared with the values obtained from correlations available in the literature for smooth duct namely Shah and London set of equations [10] and modified Blasius equation [10]. The Nusselt numbers have a maximum deviation of 5.86% while the maximum deviation of the friction factor is 2.63% from the predicted values by the Shah and London and Blasius equations, respectively.

Data reduction

The experimental data was used to determine the desired parameters as given below. All the properties of air, viz. density, viscosity, specific heat used in the calculation, were evaluated at the arithmetic mean of the inlet and the outlet temperature of air. The heat transfer rate, Q_{air} to the air can be determined as:

$$Q_{air}=\dot{m}c_p(T_{out}-T_{in}) \tag{1}$$

The local heat flux from the wall to the flowing fluid, q (assumed uniform on all surfaces which bound the porous medium) obtained from:

$$q=Q_{air}/A_s \tag{2}$$

where A_s is the heat transfer area m^2.

The average Nusselt number based on the hydraulic diameter $\overline{Nu}_{D_h}$ was evaluated in accordance with the following equation:

$$\overline{Nu}_{D_h}=\frac{qD_h}{(\overline{T}_s-T_m)k_{air}} \tag{3}$$

where hydraulic diameter D_h is,

$$D_h=\frac{4A_c}{P} \tag{4}$$

A_c and P are cross-sectional area and the wetted perimeter of the test section respectively.

The average surface temperature $\overline{T}_s$ can be calculated from the 20 points of the local surface temperatures, which can be expressed as

$$\overline{T}_s=\frac{\sum T_s}{20} \tag{5}$$

and the average air temperature T_m is given by,

$$T_m = \frac{T_{out} + T_{in}}{2} \quad (6)$$

The modified Fanning friction factor f_{D_p} (the ratio of the wall shear stress at channel to the flow kinetic energy) and the modified Reynolds number Re_{D_p} [11] are defined as

$$f_{D_p} = \frac{\Delta p}{L_0} \frac{D_p}{\rho u^2} \frac{\varepsilon^3}{(1-\varepsilon)} \quad (7)$$

$$\frac{\mathrm{Re}_{D_p}}{1-\varepsilon} = \frac{D_p \rho u}{\mu} \quad (8)$$

where the equivalent spherical diameter D_p, is the characteristic length of woven metal screens (shown in table 1) and defined as $D_p = 6/S_V$ (S_V, is the surface area per unit volume of solid phase).

UNCERTAINTY ANALYSIS

Employing the method suggested by Schultz and Cole [12], uncertainty or error analysis in the various parameters has been estimated as below:

Heat transfer coefficient (h)	±11.15%
Nusselt number ($\overline{Nu}_{D_h}$)	±11.04%
Friction factor (f_{D_p})	±6.14%

RESULT AND DISCUSSION

Average Nusselt number results

The variation of the average Nusselt number ($\overline{Nu}_{D_h}$) versus the Reynolds number (Re_{Dh}) for three studied porous media, is shown in Figure 3. It was observed that the value of average Nusselt number increases with the increase in Reynolds number. It can also be observed that the effect of Reynolds number on Nusselt number decreases, at higher Reynolds numbers. As seen in the Figure 3, the effect of Reynolds number (Re_{Dh}) on average Nusselt number decreases for third porous medium when Re reaches the value of 2100, and a similar trend occurs for second and first porous medium when Re reaches the value of 1900. Another aspect demonstrated in Figure 3 is that the porosity has an important influence on the average Nusselt number. If the porosity decreases from 0.98 to 0.97, the average Nusselt number increases between 13% and 20% depending on Reynolds number. However, average Nusselt number increases up to 50% when the porosity is decreased from 0.98 to 0.95. This appears to be due to a higher level of unsteady created in the flow as the porosity decreased and the flow passages become more tortuous and narrower with a higher solidity of such matrices.

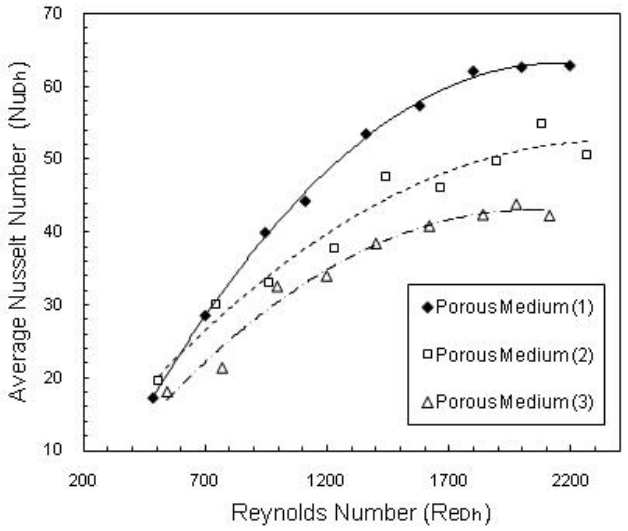

Figure 3 Effects of Reynolds number on average Nusselt number for 3 studied porous media.

Pressure drop results

The variation of the pressure drop (Δp) versus the Reynolds number (Re_{Dh}) for three studied porous media, is shown in Figure 4. It was observed that the higher the Reynolds number, the higher the pressure drop. It can also be observed from Figure 4 that the value of pressure drop increases monotonically with a decrease in porosity. If the porosity decreases from 0.98 to 0.97, the pressure drop (Δp) increases between 50% and 150% depending on Reynolds number. However, pressure drop (Δp) increases up to 200% when the porosity is decreased from 0.98 to 0.95.

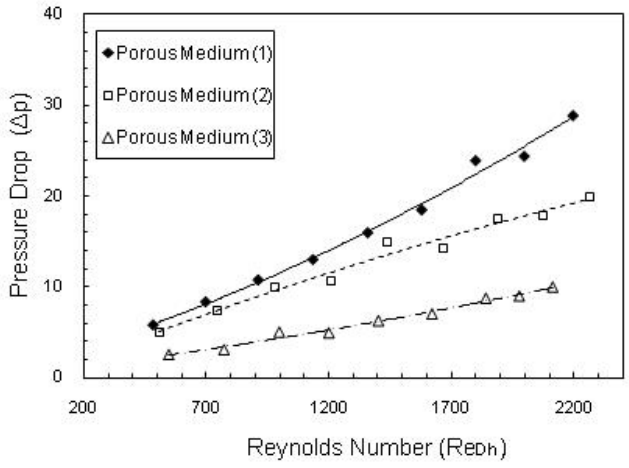

Figure 4 Effects of Reynolds number on pressure drop for 3 studied porous media.

Development of correlation

The modified Fanning friction factors f_{D_p} of the three porous media used in this study were determined following the definition given in equation (7) and plotted as functions of $\mathrm{Re}/(1-\varepsilon)$ in Figure 5. In this figure, it is noted that f_{D_p} decreases with the increase of $\mathrm{Re}/(1-\varepsilon)$. It should also be noted that the data for the three porous media fell well into a single curve.

Jones et al. [13] analyzed the pressure drop characteristics of granular porous materials. The equation is given below:

$$f_{D_p} = 150\frac{1-\varepsilon}{\mathrm{Re}_{D_p}} + 3.89\left(\frac{1-\varepsilon}{\mathrm{Re}_{D_p}}\right)^{0.13} \tag{9}$$

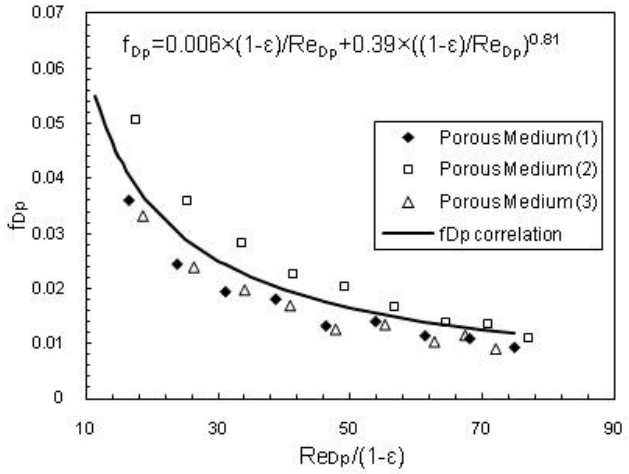

Figure 5 Correlation between f_{D_p} and $\mathrm{Re}_{Dp}/(1-\varepsilon)$.

In order to develop a correlation for pressure drop characteristic of flow through woven metal screens (Table 2), this study adopts a general equation in the form of equation (9), given below in equation (10).

$$f_{D_p} = \alpha\frac{1-\varepsilon}{\mathrm{Re}_{D_p}} + \beta\left(\frac{1-\varepsilon}{\mathrm{Re}_{D_p}}\right)^{\gamma} \tag{10}$$

A series of experiments were conducted to determine the coefficients α, β, and γ of equation (10). Based on the measured pressure drops of three woven metal matrices, present study developed an empirical equation of friction characteristic for woven metal screens. As shown in Figure 5, the correlation for the three porous media was determined to be

$$f_{D_p} = 0.006\frac{1-\varepsilon}{\mathrm{Re}_{D_p}} + 0.39\left(\frac{1-\varepsilon}{\mathrm{Re}_{D_p}}\right)^{0.81} \tag{11}$$

Table 2
Properties of metal screens

Dimension of screen (m)	Mass of a single screen (kg)	Thickness of a single screen (m)	Diameter of warp wire (m)	D_P (m)	Woven density (wires/in.)
0.4×0.04	23.77×10^{-3}	0.85×10^{-3}	0.45×10^{-3}	2.45×10^{-3}	17

Figure 6 shows the comparison of equation (11) with the experimental data (obtained from this study) of the metal screens of the plain square type. Figure 6 shows that data from present study all fall within ±25% of equation (11).

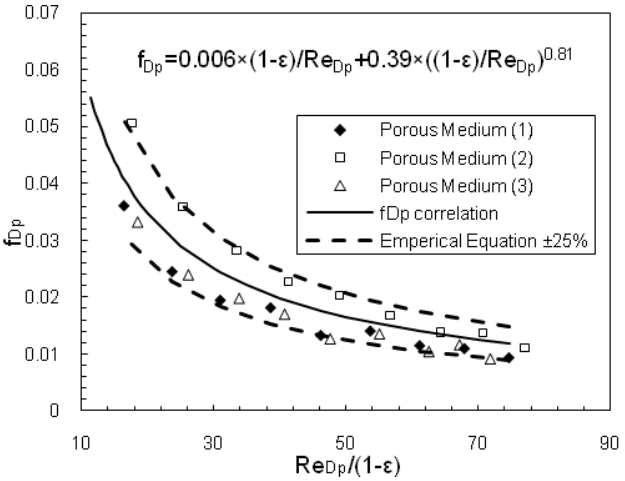

Figure 6 Deviation between experimental data and the correlation.

CONCLUSION

In this study, an experimental setup was established for data collection on heat transfer and fluid flow characteristics of air through woven metal screens. It is shown that higher heat transfer rates are achieved when using porous inserts at the expense of a reasonable pressure drop, which depends on the permeability of the porous media.

Based on the measured pressure drops of three porous matrices, this study developed an empirical equation of friction characteristic for plain-square-type metal screens. The empirical equation is:

$$f_{D_p} = 0.006\frac{1-\varepsilon}{\mathrm{Re}_{D_p}} + 0.39\left(\frac{1-\varepsilon}{\mathrm{Re}_{D_p}}\right)^{0.81} \quad f_{D_p} = \alpha\frac{1-\varepsilon}{\mathrm{Re}_{D_p}} + \beta\left(\frac{1-\varepsilon}{\mathrm{Re}_{D_p}}\right)^{\gamma}$$

where

$$f_{D_p} = \frac{\Delta p}{L_0}\frac{D_p}{\rho u^2}\frac{\varepsilon^3}{(1-\varepsilon)}, \qquad \frac{\mathrm{Re}_{D_p}}{1-\varepsilon} = \frac{D_p\rho u}{\mu} \qquad \textit{and} \qquad D_p = 6/S_V$$

REFERENCES

[1] Kays, W.M. and London, A.L., Compact Heat Exchangers, McGraw-Hill, 1964.

[2] S.Y. Kim, J.W. Paek, B.H. Kang, Flow and heat transfer correlations for porous fin in a plate-fin heat exchanger, ASME J. Heat Transfer 122 (2000) 572–578.

[3] David Edouarda, Maxime Lacroixa, Cuong Pham Huua, Francis Luckb, Pressure drop modelling on SOLID foam: State-of-the art correlation, Chemical Engineering Journal 144 (2008) 299–311.

[4] C.T.Hsu, H.L.Fu, and P.Cheng. On pressure-velocity correlation of steady and oscillating flows in regenerators made of wire-screens. *ASME J. Fluids Eng.*121:52–56, 1999.

[5] C.T.Hsu and H.Fu. Measurements of pressure drop of high frequency oscillating flows through a packed column made of wire-screens, 2004 (in manuscript).

[6] A. A. Mohamad, High efficiency solar air heater, Solar Energy 60 (1997) No. 2, 71-76

[7] G. Alvarez, J. Arce, L. Lira, M.R. Heras, Thermal performance of an air solar collector with an absorber plate made of recyclable aluminum cans, Solar Energy 77 (2004) 107–113.

[8] Varshney, L., Saini, J.S., 1998. Heat transfer and friction factor correlations for rectangular solar air heater duct packed with wire mesh screen matrices. Solar Energy 62 (4), 255–262.

[9] D.Y. Lee, K. Vafai, Analytical characterization and conceptual assessment of solid and fluid temperature differentials in porous media, Int. J. Heat Mass Transfer 42 (1999) 423–435.

[10] Rohsenow, W. M., and Hartnett, J. P. (1973).Handbook of Heat Transfer, McGraw-Hill.

[11] Ergun S., Fluid flow through packed columns, Chem. Eng.Prog. 48 (1952) 89–94.

[12] Schultz, R.R., and Cole, R., Uncertainty analysis in boiling nucleation, AIChE Symp. Series 75 (1979), 32-38.

[13] Jones D.P., Krier H., Gas flow resistance measurements through packed beds at high Reynolds numbers, J. Fluids Eng. 105 (1983) 168–173.